MicroMAS: A First Step Towards a Nanosatellite Constellation for Global Storm Observation

William J. Blackwell, G. Allen, C. Galbraith, R. Leslie, I. Osaretin, M. Scarito, Mike Shields, E. Thompson, D. Toher, D. Townzen, A. Vogel, R. Wezalis
Lincoln Laboratory, Massachusetts Institute of Technology
244 Wood St., Lexington, MA 02420-9185 U.S.A; 781-981-7973
wjb@LL.MIT.EDU

Kerri Cahoy, David W. Miller, Anne Marinan, Ryan Kingsbury, Evan Wise, Sung Wook Paek, Eric Peters, Meghan Prinkey, Pratik Davé, Brian Coffee
Space Systems Laboratory, Massachusetts Institute of Technology
77 Massachusetts Ave., Cambridge, MA 02139
kcahoy@mit.edu

Neal R. Erickson, University of Massachusetts, Amherst, MA
Department of Astronomy, University of Massachusetts at Amherst
10 North Pleasant St., Amherst, MA 01003-9305
neal@astro.umass.edu

ABSTRACT

The Micro-sized Microwave Atmospheric Satellite (MicroMAS) is a dual-spinning 3U CubeSat equipped with a nine-channel passive microwave spectrometer observing near the 118.75-GHz oxygen absorption line. The focus of this first MicroMAS mission is to observe convective thunderstorms, tropical cyclones, and hurricanes. The payload, housed in the "lower" 1U of the dual-spinning 3U CubeSat, is mechanically rotated approximately once per second as the spacecraft orbits the Earth, resulting in a cross-track scanned beam with a FWHM beamwidth of 2.5 degrees and an approximately 20-km diameter footprint at nadir incidence from a nominal altitude of 400 km. The MicroMAS flight unit is currently being developed by MIT Lincoln Laboratory, the MIT Space Systems Laboratory, the MIT Department of Earth and Planetary Sciences, and the University of Massachusetts-Amherst Department of Radio Astronomy for a 2013 launch on the Cygnus-2 ISS resupply mission.

INTRODUCTION AND MISSION OVERVIEW

Accurate monitoring and forecasting of severe weather provides enormous societal and economic benefit. High revisit-rate measurements provided by infrared (IR) imagers and sounders on satellites operating in geostationary orbit have proven to be a critically important asset. These observations, however, are blind to the most important meteorological phenomena relevant to severe weather events—clouds and the underlying precipitation. A low-Earth orbiting (LEO) constellation of passive microwave sensors could provide all-weather observations with revisit rates of approximately 30 minutes for advanced forecasting and nowcasting techniques and applications that are needed to study full hydrologic cycle processes.

The goal of the MicroMAS mission is to demonstrate a core element of the constellation at very low cost – a 3U cross-track-scanning CubeSat hosting a microwave spectrometer with nine channels near the 118.75-GHz oxygen absorption line for sensing of temperature and precipitation at approximately 20-km spatial resolution with full Nyquist sampling. MicroMAS will launch on the Cygnus-2 ISS resupply mission, currently scheduled for December 8, 2013. The CubeSat will be delivered to the ISS as Cygnus cargo and will be deployed from the Japanese Experiment Module (JEM) Small Satellite Orbital Deployer (J-SSOD). J-SSOD is capable of launching small satellites from the station using the JEM Remote Manipulator System. MIT has contracted with SpaceFlight Services and NanoRacks to provide this service. The initial orbit altitude will be approximately 400 km, and MicroMAS will decay to 300 km in approximately 75 days. Orbit inclination will be 51.6 degrees. Spacecraft de-tumbling, initial checkout, and radiometer calibration and validation will occur in the first 30 days of the mission. The NASA Wallops Flight Facility will provide ground segment services in collaboration with the Utah State University

Space Dynamics Laboratory, which has extensive UHF communications experience with the DICE CubeSat mission [1].

The relatively low cost of CubeSat remote sensing to be demonstrated by MicroMAS facilitates the deployment of a constellation of sensors, spaced equally around several orbit planes. Constellation simulations show that approximately 20 satellites could provide average revisit times approaching 30 minutes in the tropics and midlatitudes, a revolutionary step forward for atmospheric sounding and precipitation science. A small fleet of Micro-sized Microwave Atmospheric Satellites could yield high-resolution global atmospheric profiles, as well as cloud microphysical and precipitation parameters.

Significant advancements have been made in each subsystem of the MicroMAS design, which is currently in the Integration and Test phase of the project development lifecycle. Custom avionics interface boards have been designed and fabricated and are currently undergoing testing. Avionics components have undergone radiation tests [2], and the flight software architecture has been designed for a Pumpkin CubeSat Motherboard with a Microchip PIC24F microcontroller as the flight computer running Pumpkin's Salvo Real Time Operating System. The power subsystem has been upgraded to include additional body-mounted solar panels with the 2U double-sided deployables from Clyde Space. The fidelity of the attitude determination and control system (ADCS) has continued to improve via modeling, simulations, and hardware-in-the-loop testing of the satellite's unique dual-spinning, zero angular momentum LVLH-stabilized flight design. New ADCS testing facilities were designed and constructed, combining the orbit environment simulation capabilities of a Helmholtz cage and a three-axis air bearing. Spacecraft components are currently undergoing thermal-vacuum tests in order to verify the results of thermal modeling analyses. The structural design has moved to a custom, in-house chassis design, resulting in new finite-element analyses and fabrication tests, and an engineering design model of the "scanner assembly" (another in-house design incorporating a brushless DC zero-cogging motor, an optical encoder and disk, shielded bearing, and a slipring in an aluminum housing) has been assembled and is undergoing test. Full system integration of the Space Vehicle will take place in August 2013. In this paper, we describe the spacecraft bus and associated subsystems and the radiometer payload.

MICROMAS BUS

Overview

MicroMAS is a 3U CubeSat consisting of a 2U bus and 1U payload, together referred to as the "space vehicle". The 2U bus contains all spacecraft supporting subsystems as well as a scanner assembly that spins the 1U radiometer payload at 0.8 Hz. MicroMAS flies in a "space-dart" formation with four double-sided 2U solar panels deployed at 120 degrees, as shown in Figure 1. The attitude determination and control system (ADCS) uses the x reaction wheel primarily to cancel out the angular momentum of payload scanner assembly. The scanner assembly consists of an Aeroflex Z-0250-050-3-104 brushless DC zero-cogging motor equipped with an Elmo Hornet motor controller, a MicroE M1500V encoder, and a MicroE 301-00075 rotary grating. The radiometer antenna beam is scanned across the Earth's surface and through cold space (for calibration). As shown in Figure 2, the 2U bus stack also houses the MAI-400 ADCS three-axis reaction wheel assembly, the ClydeSpace CS-XUEPS2-60 electrical power system (EPS) and 20 W-hr battery, the L-3 Communications Cadet Nanosatellite UHF radio board, two custom avionics interface boards (top and bottom), and the Pumpkin PIC24F256GB210 microcontroller board and pluggable processor module (PPM). The solar panel assembly, consisting of four 2U body panels and four double-sided deployed 2U panels and monopole tape-spring antenna are also mounted to and deployed from the 2U bus.

Attitude Determination and Control

In order to maintain operational mode attitude as shown in Figure 1, the spacecraft maintains zero angular momentum with a dual-spinner. The analysis leading to the decision to implement a dual-spinner zero angular momentum system is discussed in detail in [3, 13].
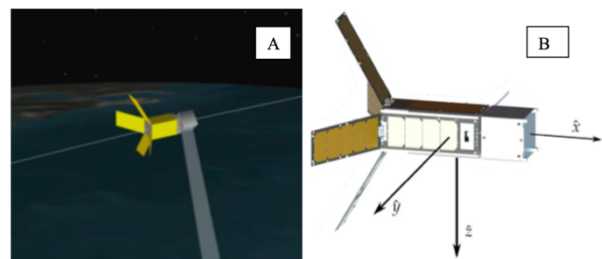
Figure 1: The dual-spinning 3U MicroMAS CubeSat with 1U payload and 2U bus. (a) Shown using AGI's STK with payload in operational mode. (b) Shown in body-centered frame as SolidWorks CAD model with representative payload module, ClydeSpace 2U body and double-sided deployed panels at a 120° angle.
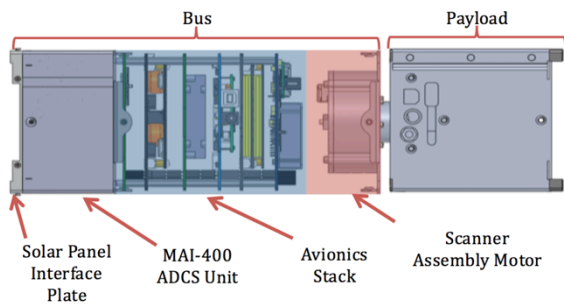
Figure 2: MicroMAS bus stack rendered using SolidWorks. The avionics stack includes custom bottom and top interface boards, ClydeSpace EPS, L-3 Communications Cadet UHF nanosatellite radio and carrier board, Pumpkin motherboard and PPM, ClydeSpace 20 W-hr battery, and scanner assembly. The monopole spring-tape antenna is not shown here.

The 1U radiometer payload continuously spins at a rate of 0.8 Hz, and the ADCS both cancels the momentum induced by the scanner assembly spinning the 1U, 1 kg payload as well as maintains orbit stability with one face of the 2U bus nadir-pointing. This requires active attitude determination and control, using a combination of sensors and actuators. The actuators on MicroMAS are three orthogonally mounted miniature reaction wheels by Maryland Aerospace Inc. (MAI-400), which include a set of torque rods to enable magnetic momentum dumping. This reaction wheel assembly was chosen because of its momentum storage capability compared to other COTS options. The MAI-400 reaction wheels have angular momentum storage capability of 11.8 mNms compared to a requirement of 6.2 mN·m·s (derived from payload inertia of 1.224×10^{-3} kg·m2 and spin rate of 0.8 Hz). The ADCS sensors include a 3-axis magnetometer (RM3000), an Analog Devices ADIS16334 six degree of freedom (DOF) inertial measurement unit (IMU), Silonex SLCD-61N8 photodiodes used as coarse sun sensors, and Excelitas TPS334 fine (6° FOV) and coarse (60° FOV) thermopiles as static Earth horizon sensors (EHS).

ADCS modes

MicroMAS has three main operational ADCS modes: Detumble, Slew, Stabilization, and Safe modes. In Detumble, the satellite will slow itself to a rate of less than 1 degree per second rotation using a B-dot control law. This consists of using the magnetometer to sense the rate of change of the Earth's magnetic field, and using the torque rods to dump momentum so that the satellite is no longer tumbling, but left in an arbitrary attitude.

After achieving less than 1 degree per second rotation, as measured using the IMU gyroscope, the satellite will switch into Slew mode. The objective of Slew mode is to slew the satellite from its arbitrary attitude after detumble into an attitude where the correct body panel is nadir-pointing and the satellite is oriented correctly along-track as shown in Figure 1. Slew mode uses the MAI-400's TRIAD [4,5] method of comparing two independent vector measurements with two reference vectors, and combining these to find the satellite's attitude in the body frame. The two vector inputs in Slew mode are the magnetometer and sun sensor vectors. The magnetometer vector will use a truncated IGRF-11 model of the Earth's magnetic field with 2010 coefficients, based on the altitude of the orbit and location in the orbit, as the reference vector. The sun sensor will use a coarse sun model from an astronomical almanac as a reference vector. The quaternion provided by TRIAD is run through an Extended Kalman Filter (EKF) in the flight processor. The EKF helps to filter much of the noise from the sensor measurements in order to make a more accurate prediction of attitude determination. The attitude estimate largely depends on the gyro measurements, and attitude measurements correct the estimate of the gyro bias. Slew mode uses the reaction wheels as the primary actuators, and uses the torque rods, which are duty cycled for operation with the reaction wheels, to dump excess momentum as continuously as possible. During slew mode, the Earth horizon sensors report telemetry, and slew mode is complete when lock on the Earth's limb is achieved.

Earth limb lock enables the transition to Stabilization mode, where the satellite again uses the TRIAD method for attitude determination using the magnetometer and Earth horizon sensors for the two vector measurements, and again the sensor inputs are run through an EKF. Throughout these modes, the *x* reaction wheel will spin at a constant speed of approximately 8000 rpm to counter the rotation of the spinning payload. This limits the momentum capabilities of the satellite, but modeling and simulation have shown that MicroMAS can determine its attitude within 20 arcminutes and maintain control within 30 arcminutes even with this limitation [3].

The reason that the EKF does not ingest each sensor measurement separately is that the MAI-400 already uses the TRIAD method to combine these data before providing a single-frame attitude estimate to the filter. Using a distributed filter offloads a significant amount of computation from the spacecraft's primary flight computer at the cost of accuracy, redundancy, and filter optimality. A distributed filter of this sort is also planned for use with ExoplanetSat [6].

Additionally, rather than using a mathematical model of the system dynamics to propagate the spacecraft's attitude between measurements, the filter further reduces the computational burden by using rate measurements from a MEMS gyroscope for attitude propagation. A complementary filter for spacecraft attitude quaternion estimation was first used in the Multimission Modular Spacecraft in 1978 [7] and described by Lefferts, Markley, and Schuster in 1982 [8]. Crassidis and Junkins extended the algorithm to the discrete–discrete case [9] using the power series approach given by Markley [10]. MicroMAS uses the discrete–discrete implementation.

ADCS test description

The MicroMAS ADCS testbed, shown in Figure 3 and described in detail in [12], is equipped to capture and test the actuator and sensor functionality of the CubeSat. The test rig is equipped with the MAI-400 reaction wheel assembly, six coarse sun sensors, the majority of the avionics stack, the scanner assembly, a mass and inertia mockup of the radiometer payload, and six fine mass adjusters for the purpose of centering the testbed's mass with its center of rotation. The MAI-400 reaction wheel assembly includes three orthogonal reaction wheels, tachometers, two sets of infrared thermopile static Earth sensors (one mounted facing in the anti-velocity direction, and one side-looking), and an analog-to-digital interface for six coarse sun sensors.

The avionics stack for the testbed includes engineering models of the bottom and top custom interface boards, a motherboard with the PIC24F microcontroller, a MHX Microhard S-band modem and radio (for lab test only), and a ClydeSpace EPS with batteries. The specific objectives of the testbed include demonstrating rate damping (determining torque coil magnetic dipole and torque produced, and comparing MAI-400 IMU tumbling rates to an external vision sensor), testing slew rates, and determining attitude determination and control accuracy and rate control of the testbed operating in stabilization mode compared with simulation predictions. In addition, transient torques and their effect on attitude determination and control accuracy of operation in stabilization mode while spinning the payload up from zero rotation will be determined. The testbed does have some limitations in its drag environment, gravity gradient torque, and limitations on range of slew (30 degrees in two horizontal axes) compared to simulation and expected on-orbit behavior.
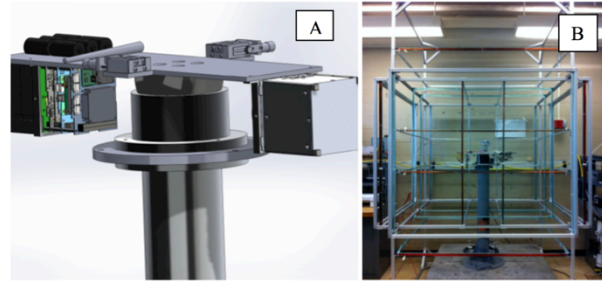
Figure 3: MicroMAS ADCS testbed. (a) SolidWorks rendering of the air bearing assembly, including micrometer stages for balancing. (b) Merritt 4-coil Helmholtz cage surrounding the 3-axis air bearing at the MIT Space Systems Laboratory.

Power

As shown in Figure 1, MicroMAS generates power using body-mounted and double-sided deployed solar panels. All the panels are 2U in length with 4-5 cells on each face. The deployed panels have cells on both sides and all four are deployed at a 120-degree angle. For the expected initial orbit of 402 x 424 km with 51.6° inclination, the satellite will nominally see 36 minutes in eclipse and 57 minutes in daylight (5568 sec per orbit). On average, the solar panels can generate up to 14.5 W. Energy is stored onboard using secondary 20 W-hr lithium polymer batteries. A ClydeSpace EPS (CS-XUEPS2-41) monitors the solar panels and batteries, collects generated power and regulates battery charging. Simulated power consumption is shown in Figure 4a and solar power generation is shown in Figure 4b. Approximately 12.6 W-hr per orbit is required by the spacecraft.
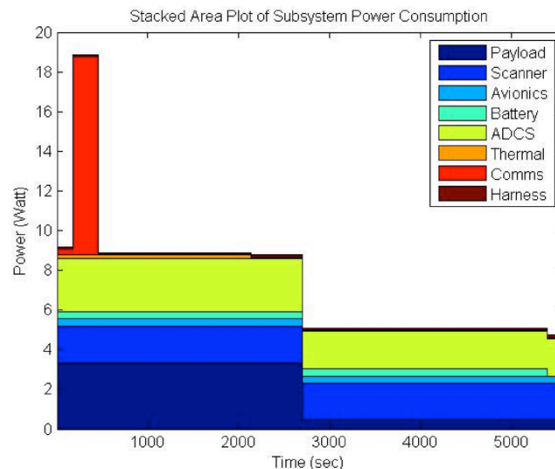
Figure 4a: MicroMAS simulated power consumption by subsystem over one orbit for nominal science operations.
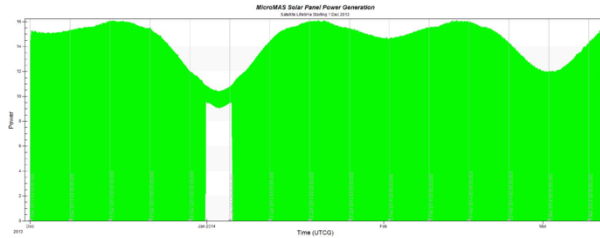
Figure 4b: MicroMAS solar power generation over the expected lifetime (from ISS orbit, epoch December 1, 2013).

Power regulation for individual components is done using custom circuitry on two avionics interface boards. Since their arrival on January 24, 2013, the team has monitored the batteries and checked voltages every two weeks to ensure that they remain above the suggested threshold for the duration of their expected shelf life. The power system will be tested with a sun simulator and representative satellite load to compare the expected system performance with simulation results. The payload will operate in a 50% duty cycle during nominal science operations to keep the power and energy draw below the desired battery depth of discharge (30%) and solar power generation capabilities. The payload will be operated as continuously as possible (e.g., on for half an orbit and off for half an orbit) to maximize science return. The maximum battery depth of discharge is expected to be 30.4%, which occurs if the payload operates throughout eclipse. The power generation capability is affected by variation in the Right Ascension of the Ascending Node (RAAN), which varies through the mission lifetime as shown in Table 1. For example, for the ISS orbit, the RAAN varies from 0—360° in about 70 days.

Table 1: Page Generation Capability as a Function of RAAN for the 402 x 425 km, 51.6° orbit, 5568 sec.

RAAN (deg)	Orbit Avg. Power (W)	Generated Energy (W-hr)
0	8.64	13.36
60	8.80	13.60
120	8.59	13.28
180	10.54	16.30
240	8.48	13.10
300	8.65	13.37

Avionics

The MicroMAS avionics design incorporates a mix of COTS and custom components. The avionics architecture is largely based on the CubeSat Kit (CSK) design popularized by Pumpkin Inc. The CSK architecture consists of a connectorized board stack and standardized pin mapping. To provide the mission-specific circuitry and interfaces, two custom boards were incorporated into this board stack. The on-board computer (OBC) is based on the Pumpkin Motherboard with a PIC24FJ256GB210 microcontroller.

Top interface board

The top interface board sits at the payload end of the CSK board stack. This board houses a brushless DC motor controller (Elmo Hornet), a magnetometer (PNI RM3000), an IMU with three-axis gyro (ADIS16334), temperature sensor interface circuitry, and numerous power distribution units. The power distribution units (PDUs) are compact high-side power switches that allow the spacecraft's OBC to control power to various subsystems. This board also provides the RS-422 signaling interfaces that are used to communicate with the radiometer payload. A custom packet format has been defined to transport data between the payload and bus over this connection.

Bottom interface board

The bottom interface board sits at opposite end of the CSK board stack, nearest the MAI-400 reaction wheels. The MAI-400 uses a rigid board-to-board interface connector, which requires end users to supply a custom PCB with the appropriate mating connector. The bottom interface board also provides the interface circuitry needed for the sun sensors that are installed on various body-mount and deployable solar panels. The analog outputs of the sun sensor interface circuit are routed directly to the MAI-400 for processing. The bottom interface board also includes PDUs that can be used to manage the power supplied to the MAI-400 reaction wheels.

Communications

The MicroMAS communications system draws heavily from the Utah State University and NSF Dynamic Ionosphere CubeSat Experiment (DICE) mission with a nearly identical architecture [1]. The spacecraft transceiver is the half-duplex L-3 Communications Cadet UHF Nanosatellite radio. The ground station is the NASA Wallops Flight Facility 18-meter dish equipped with the DICE radio and computer equipment. The uplink frequency is 450 MHz at ~9.6 kbps GFSK (19.2 kbps with FEC), and the downlink frequency is 468 MHz at ~1.5 Mbps OQPSK (3 Mbps with FEC). The average data rate from the payload to the bus for downlink is ~19.2 kbps. The radio includes a ~4 GB memory buffer which stores payload data and housekeeping telemetry between ground station passes. The L-3 Cadet UHF nanosatellite radio modem is not directly compatible with the CubeSat kit board stack architecture, therefore, a custom carrier card was

designed to map its data signals to the appropriate pins on the bus. Additionally, PDU circuits were added to allow the OBC to control power being supplied to the modem.

Structures

The primary MicroMAS bus structural components consist of the scanner assembly, the bus chassis, the board stack, and the spring-tape monopole antenna support structures. These components are shown in Figure 5 and described in the following subsections.
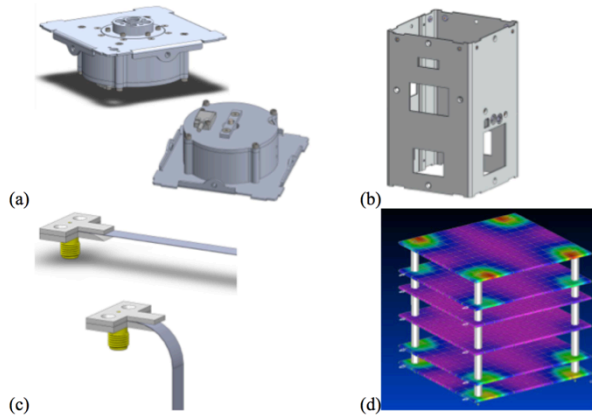
Figure 5: MicroMAS bus structural elements: (a) the scanner assembly, (b) the bus chassis, (c) the antenna structure, and (d) board stack finite element analysis.

Scanner assembly

The Scanner Assembly, shown in Figure 5a is located at the payload end of the 2U bus and facilitates the rotation of the 1U payload module. It consists of an Aeroflex Z-0250-050-3-104 brushless DC zero-cogging motor equipped with a Elmo Hornet motor controller and MicroE M1500V optical encoder and MicroE 301-00075 rotary grating for position knowledge, and a 12-wire slip ring module to transfer power and data between the bus and the payload. Due to the tight size constraints of the CubeSat platform, a custom assembly was designed, as no COTS product was found that contained all three of the above components that also fit within the 10 cm x 10 cm footprint.

Chassis

A custom chassis, shown in Figure 5b was designed to accommodate both the payload, which is externally mounted on the scanner assembly on one end, and the MAI-400 reaction wheel unit on the other end. The chassis is a solid-walled anodized aluminum structure with custom cutouts to support sensor viewing windows and solar panel connectors and circuitry.
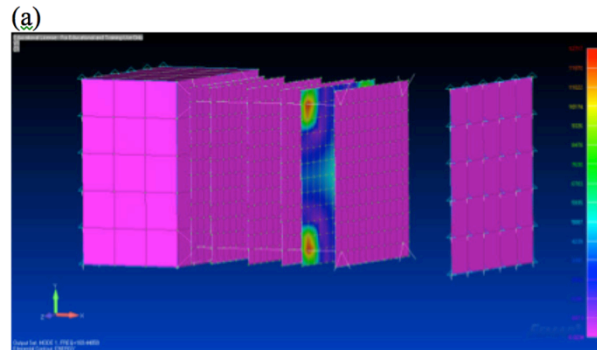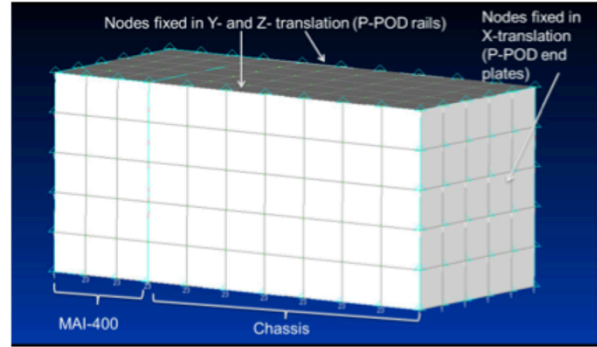
Figure 6: (a) Finite element model of full MicroMAS bus; (b) Simulation results.

Antenna structure

The antenna assembly, shown in Figure 5c, is mounted atop the bus structure in one corner of the scanner assembly cover plate. The mounting tab for the antenna fits in the gap between the 2U bus and the 1U payload, and the antenna itself is folded down on the body panel in the opposite direction of the deployable solar panels, which are folded on top of it and restrain it prior to deployment.

Avionics board stack

A three-step process was used to determine the natural frequencies of the various circuit boards in the MicroMAS electronics stack, as shown in Figure 5d. First, analytical equations were used to estimate the first natural frequencies of the individual boards. Next, simple finite element models were created for each board, using smeared masses over the entire area of the plate to represent components mounted to the boards. Then, these individual models were integrated into a single model of the entire electronics board stack. The same geometry was used for each board, with four nodes inset from the board corners constrained to represent the standoff connections and a non-structural mass applied to the entire surface of the board to represent the various components. Hexagonal beam

elements were used to model the aluminum standoffs
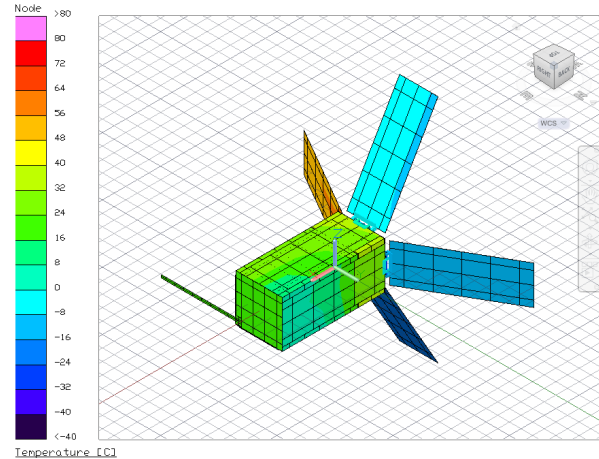
Figure 7: Thermal Desktop thermal model of the MicroMAS bus.

between each board in the stack. Four corner nodes of the bottom and top boards in the stack were pinned to represent connections to the chassis mounting plate (at the bottom) and mid-plane standoffs (at the top). The stack model is depicted in Figure 6. The first six modes of the model were of individual boards; the seventh mode of the model was the first coupled mode of the entire board stack. All modes were above the 70 Hz frequency requirement set in NASA GEVS [11].

Thermal

Thermal management for MicroMAS involves on-board temperature monitoring, passive cooling, and some heating. On-board monitoring is achieved using Innovative Sensor Technology P1K0 RTDs. Passive thermal management is used as much as possible, though several individual components require active heating, specifically those with limiting minimum operating temperature values (e.g., ClydeSpace batteries, MicroE encoder sensor). Thermal modeling was performed in Thermal Desktop, as shown in Figure 7 and summarized in Table 2.

The temperature range variation as the orbit decays is on the order of a couple of degrees. Thermal and thermal vacuum testing is underway using a three-stage approach: (1) critical components, (2) subsystem assemblies, and (3) integrated bus system. In Stage 1, thermal tests were planned for the Elmo Hornet motor controller (which was tested outside of the manufacturer's specification to check function in a high vacuum environment), the MicroE 1500V high-vacuum encoder sensor over temperature, the Excelitas (Perkin-Elmer) thermopiles being used as earth-horizon sensors in the MAI-400, and the internal thermostatically controlled heaters in the ClydeSpace batteries.

In January 2013, the motor controller was successfully tested in a vacuum environment over the expected range of operating temperatures. The MicroE encoder sensor has a minimum specified operating temperature of 0°C, which is a limiting range on spacecraft operating temperature. In March 2013, the encoder sensor was tested in a thermal chamber environment ranging from -30°C to 75°C. Some irregularities were detected in the analog output signal at low temperatures, though additional testing is needed to fully characterize the sensor's performance as a function of temperature.

Stage 2 tests are planned for the flight-like engineering model of the scanner assembly and avionics board stack, scheduled for June 2013. Stage 3 tests are planned for the full flight-model bus assembly prior to payload integration in July 2013 and consist of four cycles at spacecraft level and four cycles at subsystem and instrument level per NASA GEVS requirements.

Table 2: Model estimates of low and high temperature ranges for the MicroMAS components for 402 x 425 km 51.6° incl. orbit.

Item	Low (°C)	High (°C)
Solar panels	-60	65
MAI-400	15	33
Bottom interface board	18	39
Radio	25	42
Motherboard	20	45
EPS	19	39
Batteries	29	46
Top interface board	29	46

Budget and Risk Summary

The main cost contributors are the MAI unit, the custom ClydeSpace solar panels, and active components for the custom scanner assembly. The main technical risks associated with this mission stem from the deployed and moving components. Solar panel and antenna deployment will be tested repeatedly to ensure proper behavior on orbit. The power budget of the spacecraft is tight for the desired payload duty cycle, even with the deployed solar panels, and there is only one antenna to communicate with the ground. The balance of the payload and uniformity of the scanning assembly will also need to be well-characterized to ensure that the science-driven pointing and geolocation requirements are met.

MICROMAS RADIOMETER PAYLOAD

The radiometer is housed in a 1U (10 x 10 x 10 cm) payload section of the 3U (10 x 10 x 34 cm) MicroMAS CubeSat (see Figure 8).
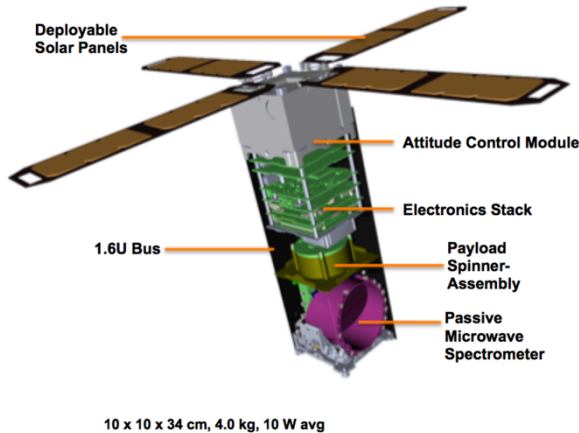
Figure 8: MicroMAS space vehicle showing the scanning radiometer payload. Note that the deployment angle of the panels has since been updated to 120 degrees as in Figure 1**. The payload fits within a 1U cube and connects to the spacecraft bus via the scanning assembly/slipring. Payload mass is less than 1 kg and average power consumption is less than 3 W.**

The payload is scanned about the spacecraft's velocity vector as the spacecraft orbits the Earth, creating crosstrack scans across the Earth's surface. The first portion of the radiometer comprises a offset parabolic reflector antenna (Figure 9), with a full-width at half-maximum (FWHM) beamwidth of approximately 2.5° at 108 GHz. Hence, the scanned beam has an approximate footprint diameter of 20 km at nadir incidence from a nominal altitude of 400 km. The antenna system is designed for a minimum 95% beam efficiency. Antenna pattern measurements have been obtained and indicate excellent performance.

The next stage of the radiometer consists of superheterodyne front-end receiver electronics with single sideband (SSB) operation (see Figure 10). The receiver front-end includes an RF preamplifier module, a mixer module, and a local oscillator (LO). The RF preamplifier module contains a low-noise RF amplifier and a weakly coupled noise diode for radiometric calibration. The mixer module comprises a HEMT diode mixer and an IF preamplifier MMIC. The 90-GHz LO is obtained using a 30-GHz dielectric resonator oscillator (DRO) and a resistive diode tripler.
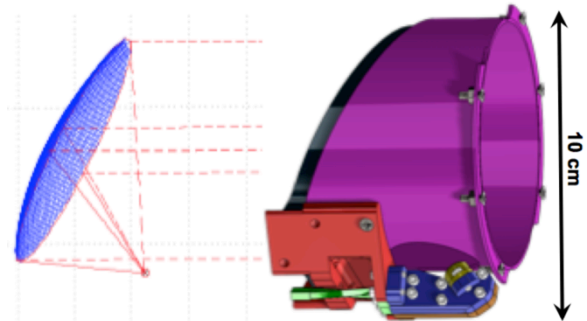
Figure 9: The MicroMAS radiometer antenna assembly comprises an offset parabolic reflector with feedhorn integrated into a waveguide assembly that mounts to the cube corner and feeds the RF front-end electronics.
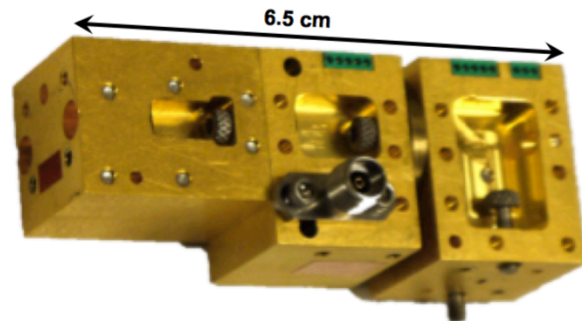
Figure 10: MicroMAS EDU receiver front-end electronics. Shown from left to right are the tripler, mixer/preamp and RF preamp/noise-diode. The flight assembly will integrate the tripler and mixer/preamp into a single block. The mass of the flight assembly will be less than 100g.

Eight channels are uniformly spaced in frequency from approximately 115 to 119 GHz, and one window channel is used at 108-109 GHz. A key technology development in the MicroMAS radiometer system is the ultra-compact intermediate frequency processor (IFP) module for channelization, detection, and analog-to-digital conversion of the incident RF energy. The IFP is shown in Figure 11.

The antenna system, RF front-end electronics, and backend IF electronics are highly integrated, miniaturized, and optimized for low-power operation. The payload also contains microcontrollers, one of which is used in the payload interface module (PIM), to package and transmit radiometric and housekeeping data to the spacecraft bus. A voltage regulator module (VRM) was also designed for the payload to convert the input bus voltage to the required voltages for the payload electronics. The payload requires 3W (average) of power. The complete radiometer payload is shown in Figure 12.
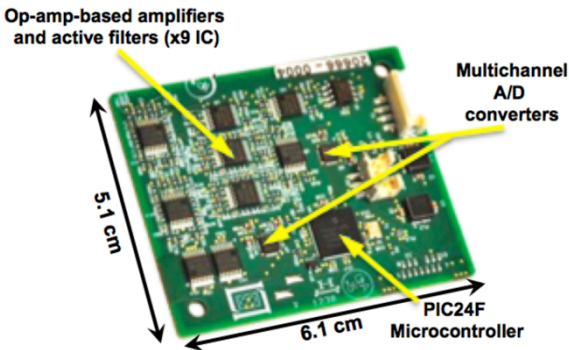
Figure 11: The MicroMAS spectrometer provides nine channels from 108-119 GHz (18-29 GHz intermediate frequency). Substrate Integrated Waveguide filters implemented in Low-Temperature Co-fired Ceramic technology are fabricated on the backside of the board. The board consumes less than 500 mW average power.
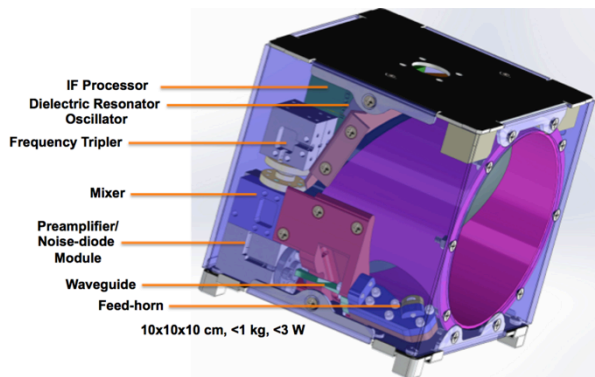
Figure 12: The complete radiometer payload assembly showing the flight version of the RF front-end electronics. The assembly has undergone vibration and environmental testing.

SUMMARY AND FUTURE PLANS

The MicroMAS mission demonstration will validate the core sensing element of a CubeSat constellation approach that could deliver multiple orders-of-magnitude cost-versus-benefit improvement relative to state-of-the-art systems. A follow-on mission, the Microwave Radiometer Technology Acceleration (MiRaTA) CubeSat mission, is scheduled for launch in 2015 into an orbit with 390-km initial altitude and 52-degree inclination. The MiRaTA CubeSat will carry out the mission objectives over a 90-day mission, including the on-orbit checkout and validation period. MiRaTA is a 3U CubeSat comprising V- and G- band radiometers (52-58 GHz, 175-191 GHz, and 206.4-208.4 GHz), the Compact TEC/Atmosphere GPS Sensor (CTAGS) with five-element patch antenna array to permit radio occultation atmospheric profiles, and relatively standard CubeSat spacecraft subsystems for attitude determination and control, communications, power, and thermal control. The spacecraft dimensions are $10 \times 10 \times 34$ cm, total mass is 4.0 kg, and total average power consumption is 6W. The cross-track scanning capabilities to be demonstrated by MicroMAS together with the multi-band radiometer and GPS radio occultation capabilities of MiRaTA could be combined into a 6U CubeSat to offer unprecedented performance at very low cost.

REFERENCES

1. Fish, C. et al., "DICE Mission Design, Development, and Implementation: Success and Challenges," Proceedings of the 26th Annual AIAA/USU Conference on Small Satellites, SSC12-XI-1, Logan, UT, 2012.

2. Kingsbury, R., F. Schmidt, K. Cahoy, D. Sklair, W. Blackwell, I. Osaretin, R. Legge, "TID Tolerance of Popular CubeSat components," accepted, to appear at IEEE NSREC, San Francisco, CA July 2013.

3. Wise, E. D., "Design, Analysis, and Testing of a Precision Guidance, Navigation, and Control System for a Dual-Spinning Cubesat," S.M. Thesis. Department of Aeronautics and Astronautics, Massachusetts Institute of Technology, Cambridge, MA, 2013.

4. Black, H.D., "A Passive System for Determining the Attitude of a Satellite," AIAA Journal, Vol. 2, July 1964, pp. 1350–1351.

5. Shuster, M.D. and S. D. Oh, "Three-Axis Attitude Determination from Vector Observations," Journal of Guidance and Control, Vol. 4, No. 1, January–February 1981, pp. 70–77.

6. Pong, C. M., et al., "High-Precision Pointing and Attitude Determination and Control on ExoplanetSat," AIAA Paper 2012-4783, Aug. 2012.

7. Murrell, J., "Precision Attitude Determination for Multimission Spacecraft," AIAA Paper 78-1248. Aug. 1978.

8. Lefferts, E. J., Markley, F. L., and Shuster, M. D., "Kalman Filtering for Spacecraft Attitude Estimation," AIAA 82-70, Jan. 1982.

9. Crassidis, J. L. and Junkins, J. L., *Optimal Estimation of Dynamic Systems*, 2nd ed, Applied Mathematics & Nonlinear Science Vol. 24, CRC Press, Boca Raton, FL, 2012, pp. 457–60.

10. Markley, F. L., "Matrix and Vector Algebra," *Spacecraft Attitude Determination and Control*, ed. James R. Wertz, Astrophysics and Space Science Library Vol. 73, Kluwer Academic Publishers, Dordrecht, the Netherlands, 1978, pp. 744–57.

11. NASA GSFC-STD-7000, Goddard Technical Standard: General Environmental Verification Standard (GEVS) for GSFC Flight Programs and Projects, April 2005.

12. Prinkey, M., D.W. Miller, P. Bauer, K. Cahoy, E.D. Wise, C.M. Pong, R.W. Kingsbury, A.D. Marinan, H.W. Lee, E. Main, "CubeSat Attitude Control Testbed Design: Merritt 4-Coil per axis Helmholtz Cage and Spherical Air Bearing," *manuscript in preparation for AIAA GNC August 2013, Boston, MA*.

13. E.D. Wise, C.M. Pong, D.W. Miller, K. Cahoy, "A Dual-Spinning, Three-Axis-Stabilized CubeSat for Earth Observations," *manuscript in preparation for AIAA GNC August 2013, Boston, MA*.